Video Article

# Mouse Model of Pressure Ulcers After Spinal Cord Injury

Suneek Kumar[1], Yuying Tan[1], Martin L Yarmush[1,2], Biraja C Dash[3], Henry C Hsia[3], Francois Berthiaume[1]

[1]Department of Biomedical Engineering, Rutgers University

[2]Center for Engineering in Medicine, Massachusetts General Hospital, Harvard Medical School, Shriners Hospitals for Children

[3]Department of Surgery, Yale School of Medicine, Yale University

Correspondence to: Francois Berthiaume at fberthia@soe.rutgers.edu

URL: https://www.jove.com/video/58188
DOI: doi:10.3791/58188

Keywords: Spinal cord injury, pressure ulcers, magnets, ulcer stages, ulcer grading, proliferation, migration

Date Published: 7/31/2018

Citation: Kumar, S., Tan, Y., Yarmush, M.L., Dash, B.C., Hsia, H.C., Berthiaume, F. Mouse Model of Pressure Ulcers After Spinal Cord Injury. *J. Vis. Exp.* (), e58188, doi:10.3791/58188 (2018).

## Abstract

Pressure ulcers (PUs) are common debilitating complications of traumatic spinal cord injury (SCI) and tend to occur in soft tissues around bony prominences. There is, however, little known about the impact of SCI on skin wound healing in the context of animal models in controlled experimental settings. In this study, a simple, non-invasive, reproducible and clinically relevant mouse model of PUs in the context of complete SCI is presented. Adult male mice (Balb/c, 10 weeks old) were shaved and depilated. Post-depilation (24 h), mice were subjected to laminectomy followed by complete spinal cord transection (T9-T10 vertebrae). Immediately after, a skin fold on the back of the mice was lifted and sandwiched between two magnetic discs held in place for next 12 h, thus creating an ischemic area that developed into a PU over the following days. The wounded areas demonstrated tissue edema and epidermal disappearance by day 3 post-magnet application. PUs spontaneously developed and healed. Healing was, however, slower in the SCI mice compared to control non-SCI mice when the wound was created below the level of SCI. Conversely, no difference in healing was seen between SCI and control non-SCI mice when the wound was created above the level of SCI. This model is a potentially useful tool to study the dynamics of skin PU development and healing after SCI, as well as to test therapeutic approaches that may help heal such wounds.

## Introduction

Pressure ulcers (PUs) are major secondary complications of traumatic SCI[1]. PUs are localized injuries to the skin and/or underlying tissues that usually occur over bony prominences where body weight is concentrated while the patient is sitting or lying[1]. The skin, fat, and muscle are exposed to this constant pressure that leads to the development of localized ischemia, tissue inflammation, mechanical damage, and necrosis[2,3].

The development of PUs is affected by several local factors, including the magnitude of pressure and shear, loading duration, skin moisture and temperature, injury longevity, and general skin hygiene. There are also systemic factors that play a role, such as general physical condition, bone and muscle tissue morphology and strength[4],patient age, hematological measures, gender, and even socio-economic factors including marital status, education, and income[4,5].

The prevention and treatment of PUs remain significant challenges in SCI patients. SCI patients develop PUs in ~30-40% of cases, with a re-occurrence rate of 60-85%, possibly due to weak scar tissue and lack of protective sensation[1]. Thus, PUs often leads to re-hospitalization of SCI patients, and overall pose a significant financial burden (80% more vs. SCI only) to the health care system[5,6,7,8,9,10].

To the best of our knowledge, there have been no studies in controlled experimental settings to investigate the impact of SCI on the PU healing process because of the lack of suitable animal models. Here, a reproducible and clinically relevant mouse model of PU in the skin is described. This model can be used to study the dynamics of PU onset and subsequent healing, as well as to test potential therapeutic approaches to prevent PU or improve PU healing in the context of SCI.

## Protocol

All animal handling and surgical procedures were performed in accordance with a protocol approved by the Rutgers University Institutional Animal Care and Use Committee. Mice were fed standard diet and water *ad libitum*.

## 1. Preparation of Surgical and Non-Surgical Instruments

1. Sterilize the surgical and non-surgical instruments in an autoclave. Clean the
2. surgical operating table with 70% ethanol and warm a heating pad to 37 °C.
3. Place the heating pad on the operating table and cover it with sterile surgical drapes.
   NOTE: In all survival procedures, the "No Touch" technique is used here to maintain sterility.

## 2. Preparation of Animals and Performing the T9-T10 Spinal Laminectomy

1. Procure adult (Balb/c) 10-week-old male mice. Induce anesthesia in each animal using an inhaler beginning with 5% isoflurane, and then decrease to 2-3% to maintain sedation for the remainder of the procedures.
2. Confirm complete anesthesia by eliciting no response to a paw/tail pinch induced nociception stimulation.
3. Shave the hair over the dorsum (head to tail) with an electric clipper, and then apply the depilatory cream (3 min) to remove the remaining hair. Finally, wash the dorsum with running water/wet scrub, and return the animals to their cages.
   NOTE: This is necessary to avoid additional irritation to the skin and chemical contamination at the time of skin wounding
4. The next day, similarly anesthetize the animals and scrub the skin with 3 alternative preparations of betadine scrub and 70% ethanol.
5. Apply ophthalmic ointment to the corneas to protect the eyes from drying during the surgical procedure.
6. With a scalpel, perform a skin incision (~1.0-1.5 cm) along the midline on the back at the level of T8-T12 vertebrae.
   Note: The level of vertebrae is identified by back counting the vertebra from T13 using the location of floating ribs that correspond to T13 vertebra[11,12].
7. Clear the subcutaneous adipose tissue to get access to the paraspinal muscles and then dissect them slowly to expose the spinous processes and laminae on both sides.
   Note: Do this procedure very carefully to avoid excess bleeding or any injury to the spinal cord, at this point.
8. Perform a laminectomy to expose the spinal cord (T9-T10 vertebrae) by gently peeling off the spinal lamina using microdissecting forceps.
   NOTE: Perform the laminectomy so that an excess of the spinal cord is exposed to facilitate the creation of the injury. In the sham control group, only the laminectomy is performed.

## 3. Performing the T9-T10 Complete Spinal Cord Injury

1. Using forceps, secure the spinal column at T8 and lift up to exaggerate the spinal curvature.
2. Using fine scissors, section the spinal cord between the T9 and T10 vertebra all the way to the floor of the vertebral canal, to ensure complete transection.
3. After observing the complete transection under a surgical microscope, apply a piece of subcutaneous fat over the laminectomy site to provide additional protection to the spinal cord prior to surgical site closure.
4. Finally, close the wound and suture the paravertebral muscles, superficial fascia, using continuous suture with non-absorbable silk. Then close the skin using suture clips[12].
5. Post-SCI, observe the bowel movement on the next day; however, manage the urinary bladder by manual bladder evacuation.
   NOTE: The Basso Mouse Scale (BMS) can be used to monitor the progress of hindlimb functional recovery post-SCI at day 2 and then weekly, see **Supplementary Figure 1**[11,12,13].

## 4. Induction of Skin Pressure Ulcer after Complete SCI

1. Immediately after the SCI surgery, scrub the back of the animal with betadine and 70% alcohol.
2. For a PU below the SCI site, inject in the dorsal skin near the sacrum, a very small volume (10 µL) of 0.125% bupivacaine solution using a 25-gauge needle at equidistant places ~0.5-1.0 cm apart, in an ellipse around the magnet application site.
   NOTE: For a PU above the SCI site, inject the dorsal skin near the cervical region.
3. Gently lift a skin fold on the back of the mouse and sandwich it between 2 magnetic discs (5×12 mm diameter, 2.4 g each, 3800 G magnetic force) (**Figure 1**).[11,12]
4. Immediately after magnet application, return animals to single cages placed onto a heating pad until full consciousness is regained (**Figure 1**).
5. After 12 h of magnet application, lightly anesthetize animal with isoflurane and remove the magnets. Take a photograph of the wound sites, to record the initial appearance of PU (day 0 time point). Cover the wound with transparent dressing film (3M) to avoid drying or contamination.

## 5. Post-Operative Animal Care, Euthanasia, and Tissue Collection for Histology

1. Immediately after surgery, inject the animal with 1 mL of 0.9% saline subcutaneously for hydration.
2. Subcutaneously inject buprenorphine-SR (1 mg/kg) immediately for analgesia.
3. Inject subcutaneously animal daily meloxicam (1 mg/kg), and cefazolin (50 mg/kg for 3-7 days), and daily manual bladder evacuation.
4. Place animals in single cages and provide accessible food and water *ad libitum*.
5. Remove surgical clips 7 days after SCI surgery.
6. At the desired time points after SCI and skin wounding, euthanize animals by $CO_2$ inhalation (3-5 min), in accordance with the AVMA Guidelines on Euthanasia[14].
7. Collect wounded skin samples, fix in 10% formalin for 24 h, and then store in 70% ethanol at 4°C until sectioning.
8. To process tissues, embed in paraffin and generate thin sections (5 µm) on a microtome. Stain with hematoxylin and eosin (H&E) to visualize tissue morphology ( **Figure 3**). For immunohistochemistry studies ( **Figure 4**), stain sections using appropriate antibodies for Ki67 (proliferation), CD31 (angiogenesis), and alpha-smooth muscle actin (α-SMA) as described in Kumar et al.[12]
   NOTE: Image analysis software can be used to quantify image features.12

## Representative Results

This protocol creates a PU in the setting of complete SCI. Briefly (as illustrated in **Figure 1**), all mice with or without complete SCI tolerated the magnets very well, which remained in their original position for the full 12 h (**Figures 1c, 1d, 1f, 1h**). All the mice developed two circular wounds separated by a bridge of normal tissue (**Figure 1e**, 1g, 1i). The initial wounding response was similar in mice without SCI (**Figure 1e**), or with SCI below the SCI site (**Figure 1g**) or above the SCI site (**Figure 1i**).

**Figure 2** depicts the disappearance of the epidermis by day 3 of post magnet removal, and its reappearance by day 7, albeit with a significantly slower migration in wounds created below the level of the SCI in SCI mice.

The pressure wounds were graded as per previously published criteria[12]. **Figure 3** and **Figure 4** depict the healing features in SCI and control non-SCI mice. The SCI group exhibited slower healing, larger scar area, thinner epidermis and dermis, and lower density of proliferating cells ($Ki67^+$ cells), blood vessels ($CD31^+$ cells), and alpha-smooth muscle actin ($\alpha\text{-}SMA^+$) in the skin wounds[11,12].

When the skin wounds were created above the level of SCI, as shown in **Figure 5**, no change in healing time, epidermal and dermal thicknesses or scar area was seen when compared to non-SCI controls.

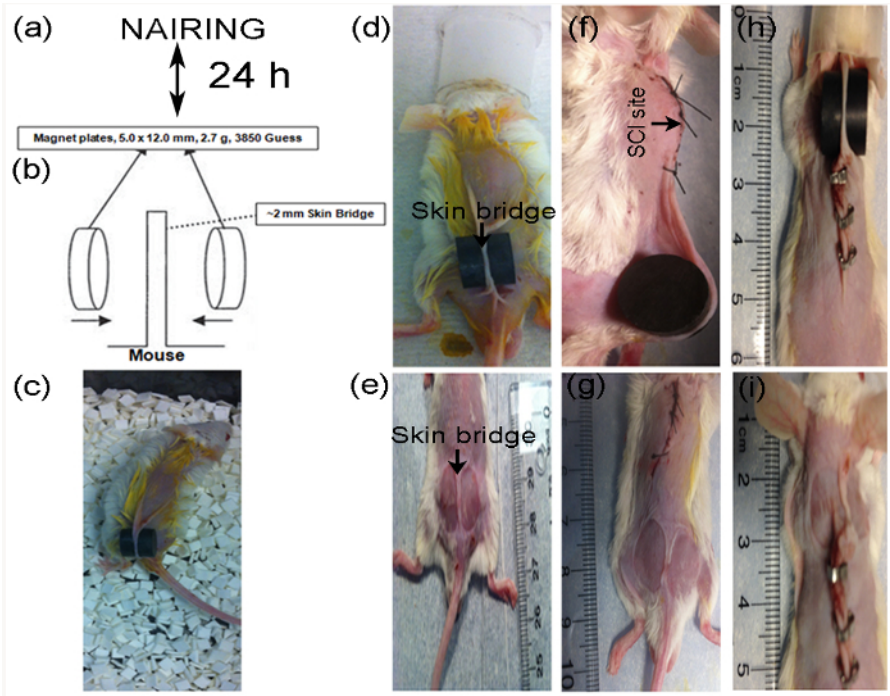


**Figure 1: Experimental procedure for creating pressure wounds in non-SCI (n=3) and complete-SCI mice (n=3).** After 1-week habituation in the laboratory, mice were shaved and depilated (a). Schematic of magnetic disc (M) placement (b, modified from Stadler *et al.*[15]). Placement of magnetic discs on skin dorsum of a normal mouse and its activity after recovery from anesthesia in the cage (d, c). In SCI mice, discs can be placed below (f) or above (h) the SCI site. The area of magnet-induced skin injury is visible immediately after 12 h of M application, which shows 2 wounds separated by an intact skin bridge in the non-SCI (e) and SCI mice (g, i). Please click here to view a larger version of this figure.

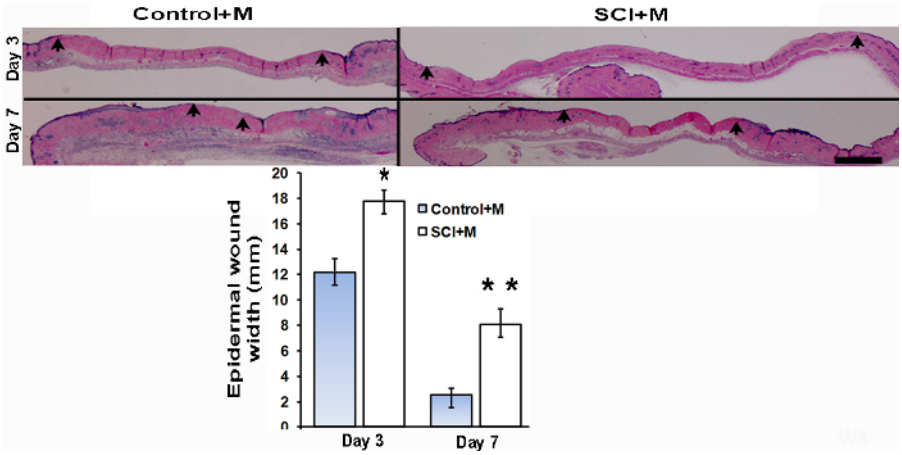


**Figure 2: Skin wound histology (H & E stain) and epidermal wound width.** On day 3 and day 7 after M application, a set of mice were sacrificed in the non-SCI (Control + M) and complete-SCI (SCI + M) groups to study the early effects M-induced ischemia and then reperfusion. Arrows indicate the epidermal wound edges, located where the epithelial lining thins out and disappears. Scale bar = 1 mm. Epidermal wound width as measured in each group (n=3 at each time point) is represented in the lower panel bar diagram. Statistical significance determined by Student t-test. *p<0.05 and **p<0.01. Data are presented as mean ± SEM (standard error of the mean). This figure has been modified with permission from the Journal of Neurotrauma, 35, 6, 815-824, (2018), published by Mary Ann Liebert, Inc., New Rochelle, NY[12]. Please click here to view a larger version of this figure.

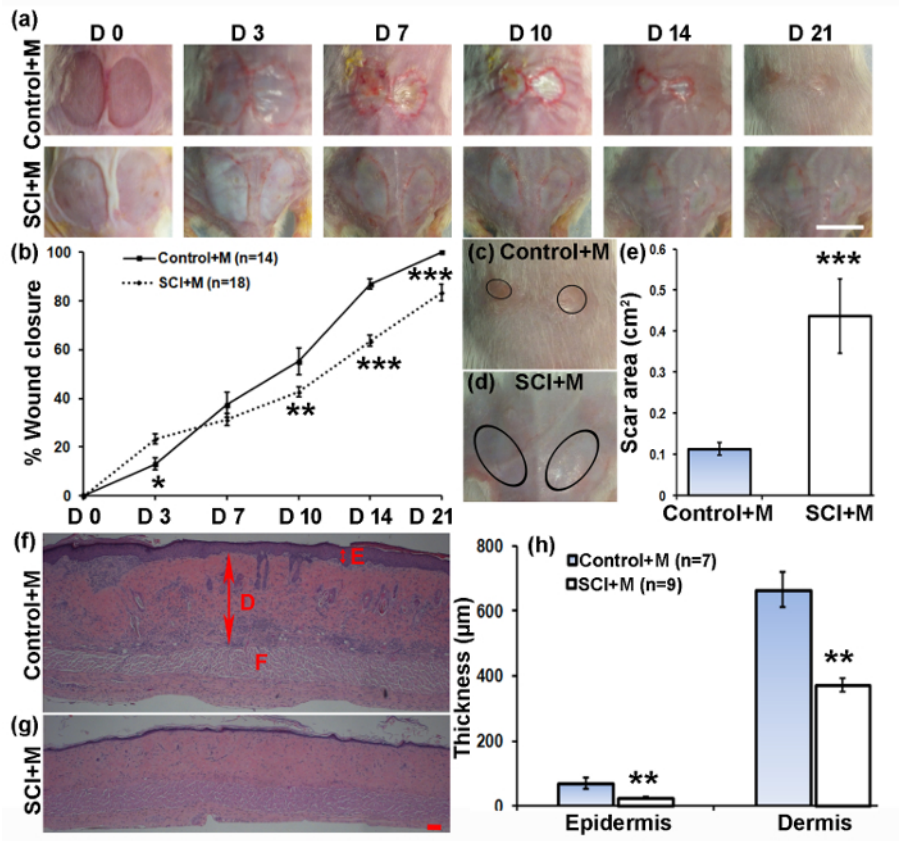


**Figure 3: Impact of complete SCI on M-induced PU development and healing.** (a) Representative images of skin wounds in non-SCI (Control + M) and complete-SCI (SCI+M) mice after PU induction over the period of 21 days. Scale bar = 1 cm. (b) Quantified wound images showing the fraction of wound closure as a function of time. (c, d) Representative images of healed wounds showing the scar area in non-SCI and SCI mice. (e) Quantified scar area in non-SCI versus SCI mice. (f, g) Representative histology of healed wound skin (H & E staining) showing epidermis (E, double arrows), dermis (D, large double arrows), and fat layer (F). Scale bar = 100 µm. (h) Quantification of epidermal and dermal thicknesses of healed wounds at time of wound closure (21 days for non-SCI, and 35 days for SCI mice). Data are presented as mean±SEM. Statistical significance determined by ANOVA followed by post-hoc Fisher's LSD test and Student's t-test. *p<0.05, **p<0.01, and ***p<0.001. This figure has been reprinted with permission from the Journal of Neurotrauma, 35, 6, 815-824, (2018), published by Mary Ann Liebert, Inc., New Rochelle, NY[12]. Please click here to view a larger version of this figure.

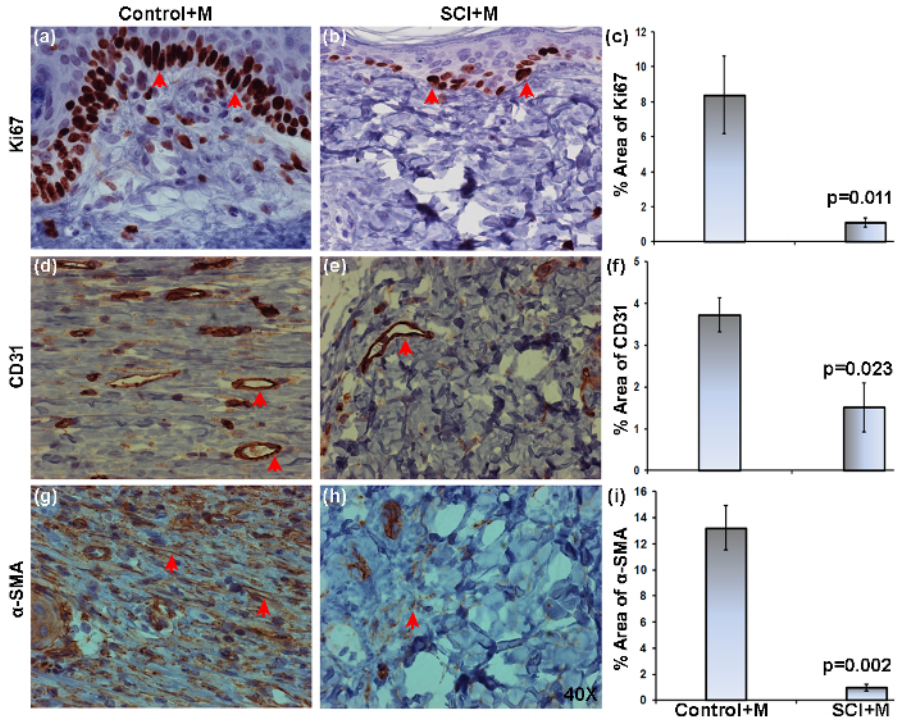


**Figure 4: Expression of Ki67, CD31, and a-SMA in skin ulcers of non-SCI and SCI mice.** Wound tissues were harvested after wound closure, namely on days 21 (Control+M) and 35 (SCI+M) post-PU induction. Representative images of 5 µm thick sections stained with anti-Ki67, anti-CD31, or anti-α-SMA and visualized with a 40X objective. Representative images of non-SCI (a, d, g) and SCI (b, e, h) mice show the distribution of $Ki67^+$, $CD31^+$, and $α\text{-}SMA^+$ (brown stain, red arrows point to some stained areas). The % positive area of expression as obtained by image analysis is compared between the groups (c, f, i). The area was averaged from three 40X fields (two from wound edges and one from wound center) per section (2/mouse, 3 mice in each group). Data are presented as mean ± SEM. Statistical significance was determined by Student's t-test. This figure has been reprinted with permission from the Journal of Neurotrauma, 35, 6, 815-824, (2018), published by Mary Ann Liebert, Inc., New Rochelle, NY[12]. Please click here to view a larger version of this figure.

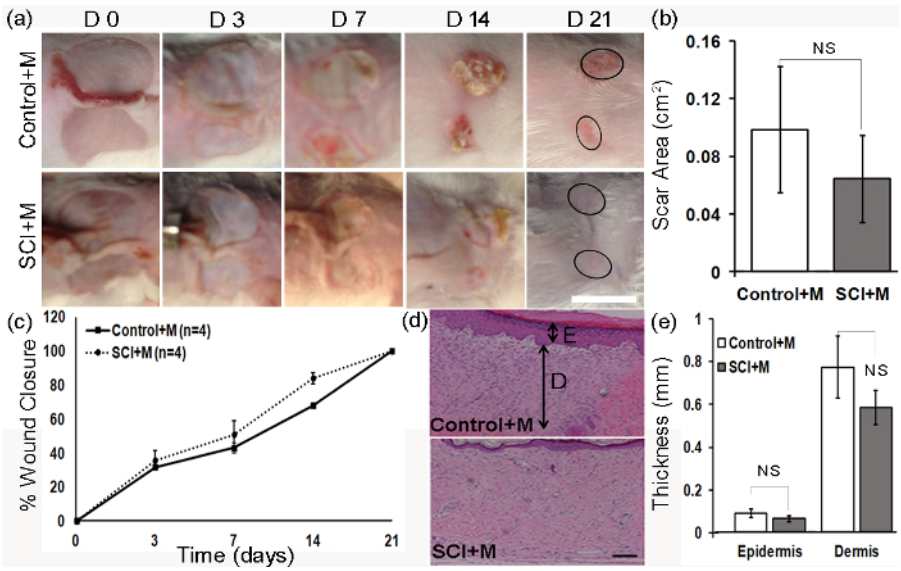


**Figure 5: Impact of SCI on development and healing of ulcers above the SCI site.** Representative images of ulcers in the non-SCI (Control + M) and SCI (SCI + M) mice over the observation period (a). Scale bar= 1 cm. The scar area on day 21 is represented by circles (a) and values were averaged in non-SCI and SCI mice (b). Quantified wound images showing the fraction of wound closure as a function of time (c). Representative histology of healed skin ulcers showing epidermis (E, small double arrow) and dermis (D, large double arrow). Scale bar = 100 µm (d). Quantification of epidermal and dermal thicknesses of healed skin ulcers at wound closure time (day 21). Data are presented as mean ± SEM. Statistical significance determined by ANOVA followed by posthoc Fisher's LSD test, or Student t-test. NS-statistically non-significant. This figure has been modified and reprinted with permission from the Journal of Neurotrauma, 35, 6, 815-824, (2018), published by Mary Ann Liebert, Inc., New Rochelle, NY[12]. Please click here to view a larger version of this figure.

**Supplementary Figure 1: Motor function in SCI mice was assessed using the BMS score on post-injury day 2 and then weekly.** The BMS score at day 2 and week 5 were 0.058±0.058 (median 0-no movement, n = 17) and 0.35±0.12 (n = 17, median-0). Data are represented as mean±SEM. This figure has been modified and reprinted with permission from the Journal of Neurotrauma, 35, 6, 815-824, (2018), published by Mary Ann Liebert, Inc., New Rochelle, NY[12]. Please click here to download this figure.

## Discussion

The protocol in this study describes a novel experimental model of PUs to evaluate the impact of SCI on wound healing. The skin PUs were induced via a 12 h application of two 12 mm diameter disc magnets on a dorsal skin fold, either set above or below the SCI site. Data show that SCI slows down skin wound healing in mice. Importantly, these observations were specifically made in skin wounds below the innervation level of the SCI, as wounds made above the SCI level, and thus that remained innervated, were largely unaffected in their healing pattern compared to the non-SCI mice.

The PU protocol described herein is based on a previously published method used in mice, where weaker magnets (1000 Gauss) were applied in three cycles of 12 h magnet application separated by 12 h without magnet[15]. Initially, we compared using one, two, and three 12 h cycles of magnet application. A disadvantage of using repeated applications is that each time special care must be taken to detach the magnet from the skin fold and reapply it at the exact same location. A single application is therefore much simpler and was sufficient to create a PU in the mouse dorsal skin fold. Otherwise, this methodology does not require a complex device, does not impair animal movements, and is very reproducible. Studies using different magnet sizes, shapes and or strengths, or attempting to create PUs in different anatomical locations may need to reoptimize the protocol. As in all skin wound healing studies, it is important to properly apply and regularly change the transparent film covering to avoid drying and contamination of the wound bed.

The mechanism of PU formation in this model relies on the compressive force between two magnets, which is expected to substantially exceed capillary and venous perfusion pressures in the skin, and has previously been well documented to induce lesions in larger animals[16]. Using a single 12 h cycle created a skin ulcer that had injury extending deep into the dermis, which corresponds to stages I and II according to standard criteria[15]. One limitation of this technique is that we were not able to get a stage III-IV PU. Therefore, one could not study the involvement of muscles and bones in PU development and healing without significant modifications to our current model. Furthermore, the PUs we generate heal spontaneously and, therefore, do not faithfully represent a chronic PU as might be seen in human patients. Interestingly, however, the method resulted in a PU of the initial similar size that closed with similar dynamics as commonly used 1 cm x 1 cm full-thickness excisional skin wounds. The PU induction method spares the underlying panniculus carnosus, while it is completely removed in the excisional model. Thus, it appears that the panniculus carnosus does not play a major role in the wound closure process, which, in mice and other rodents, primarily occurs via contraction mediated by fibroblasts and myofibroblasts in viable dermis surrounding the wound site, with little scar formation[17].

The site of PU induction, above or below SCI, does not interfere with the skin incision used to access the site of SCI. Therefore, the method can be readily applied below or above the level of SCI, which enables studies that can differentiate the local vs. systemic effects of SCI on wound healing. While non-SCI animals continue to gain weight after PU induction, the growth of SCI animals is stunted. In spite of this profound systemic change, wound healing was not affected when the PU was created above the SCI level. This model can, therefore, be used to better understand the role of the local innervation in wound healing. As in all studies that involve SCI, it is important to provide special care and monitoring to the post-SCI mice, which require manual draining of the bladder, monitoring of bowel conditions, and prophylactic antibiotic treatment[11,12].

SCI patients are substantially challenged even with the best hospital care and education, and skin PUs impart significant costs to the US healthcare system. This model allows side-by-side evaluation of the effect of SCI on skin PU development and healing, which provides a platform for testing various therapeutic strategies that may help PU healing in SCI patients.

## Disclosures

The authors have nothing to disclose.

## Acknowledgements

This work was partially supported by the New Jersey Commission on Spinal Cord Research (CSCR15IRG010), the U.S. Department of Defense (SC160029), and the Yale Department of Surgery Ohse Research Grant Program. We thank Sean O' Leary from the W.M. Keck Center for Collaborative Neuroscience, Rutgers for technical assistance.

## References

1. Rappl, L.M. Physiological changes in tissues denervated by spinal cord injury tissues and possible effects on wound healing. *International Wound Journal.* **5** (3), 435-444 (2008).
2. Salcido, R., Popescu, A., & Ahn, C. Animal models in pressure ulcer research. *The Journal of Spinal Cord Medicine*. **30** (2), 107-116 (2007).
3. Mak, A.F., Zhang, M., & Tam, E.W. Biomechanics of pressure ulcer in body tissues interacting with external forces during locomotion. *Annual Review of Biomedical Engineering.* **12**, 29-53 (2010).
4. National Pressure Ulcer Advisory Panel, European Pressure Ulcer Advisory Panel, and Pan Pacific Pressure Injury Alliance. *Prevention and Treatment of Pressure Ulcers: Clinical Practice Guideline.* Osborne Park, Western Australia: Cambridge Media (2014).
5. Marin, J., Nixon, J., & Gorecki, C. A systematic review of risk factors for the development and recurrence of pressure ulcers in people with spinal cord injuries. *Spinal Cord.* **51** (7), 522-527 (2013).
6. Krause, J.S. Skin sores after spinal cord injury: relationship to life adjustment. *Spinal Cord.* **36** (1), 51-56 (1998).

 

7. Redelings, M.D., Lee, N.E., & Sorvillo, F. Pressure ulcers: more lethal than we thought? *Advances in Skin & Wound Care.* **18** (7), 367-372 (2005).
8. Kruger, E.A., Pires, M., Ngann, Y., Sterling, M., & Rubayi, S. Comprehensive management of pressure ulcers in spinal cord injury: current concept and future trends. *The Journal of Spinal Cord Medicine.* **36** (6), 572-585 (2013).
9. Lala, D., Dumont, F.S., Leblond, J., Houghton, P.E., & Noreau, L. Impact of pressure ulcers on individuals living with a spinal cord injury. *Archives of Physical Medicine and Rehabilitation.* **95** (15), 2312-2319 (2014).
10. Li, C., DiPiro, N.D., & Krause, J. A latent structural equation model of risk behaviors and pressure ulcer outcomes among people with spinal cord injury. *Spinal Cord.* **55** (6), 553-558 (2017).
11. Kumar, S., Yarmush, M.L., & Berthiaume, F. Impact of complete spinal cord injury on neovascularization and tissue granulation in mouse model of skin pressure ulcers. *Journal of Neurotrauma.* **34** (13), A72-A73 (2017).
12. Kumar, S., Yarmush, M.L., Dash, B.C., Hsia, H.C., & Berthiaume, F. Impact of complete spinal cord injury on healing of skin ulcers in mouse models. *Journal of Neurotrauma.* **35** (6), 815-824 (2018).
13. Basso, D.M., Fisher, L.C., Anderson, A.J., Jakeman, L.B., McTigue, D.M., & Popovich, P.G. Basso Mouse Scale for locomotion detects differences in recovery after spinal cord injury in five common mouse strains. *Journal of Neurotrauma.* **23** (5), 635-659 (2006).
14. Leary, S. *et al. AVMA Guidelines for the Euthanasia of Animals.* American Veterinary Medical Association, Schaumburg, Illinois, USA (2013).
15. Stadler, I., Zhang, R.Y., Oskoui, P., Whittaker, M.S., & Lanzafame, R.J. Development of a simple, noninvasive, clinically relevant model of pressure ulcers in the mouse. *Journal of Investigative Surgery.* **17** (4), 221-227 (2004).
16. Peirce, S.M., Skalak, T.C., & Rodeheaver, G.T. Ischemia-reperfusion injury in chronic pressure ulcer formation: a skin model in the rat. *Wound Repair and Regeneration.* **8** (1), 68-76 (2000).
17. Wong, V.W., Sorkin, M., Glotzbach, J.P., Longaker, M.T., & Gurtner, G.C. Surgical approaches to create murine models of human wound healing. *Journal of Biomedicine and Biotechnology.* **2011**, 969618-969625 (2011).


 